Soft Computing
https://doi.org/10.1007/s00500-021-05621-8

FOCUS

Brain tissue volume estimation to detect Alzheimer's disease in magnetic resonance images

T. Priya[1] · P. Kalavathi[1] · V. B. Surya Prasath[2,3,4,5] · R. Sivanesan[1]

Abstract
Volume estimation of brain tissues such as the White Matter, Gray Matter and Cerebrospinal Fluid is an important task in brain image analysis and also used to diagnose neurological and psychiatric disorders. In this work, brain tissue volume reduction is estimated to detect Alzheimer's disease (AD) using magnetic resonance images. The proposed method initially applies Hue Saturation Value-Based Histogram Thresholding Technique to segment the brain tissue. After that, brain volume is estimated using the pixel counting-based method (PCBM) to detect AD. The proposed method was investigated with images obtained from T1-weighted images of cognitive normal (CN) /normal (N) and AD images from Minimum Interval Resonance Imaging in Alzheimer's Disease and Alzheimer's Disease Neuroimaging Initiative and T1- and T2-weighted real-time images collected from a medical diagnostic clinical imaging center. The estimated brain tissue volume between the AD and CN/N brain tissue clearly quantifies the brain tissue reduction and it is compared with existing automatic estimation method statistical parametric mapping (SPM). Comparing to SPM, our PCBM method accurately estimates the brain tissue volumes and can be used as a potential tool to detect AD using MR imaging data.

Keywords Alzheimer's disease · Brain tissue · Magnetic resonance imaging · Statistical parametric mapping · Pixel counting-based method · Volume estimation

1 Introduction

Medical imaging is an important field and includes applications of various techniques from mathematics, physics, statistics, engineering, biology and medicine. It deals with the evolving technologies to generate images of the internal parts of human body which are hidden by skin and bones for different clinical purposes, such as medical strategies and diagnosis or medical science including the study of normal and pathological structures. There are many radiological and diagnostic tools used to analyze the different types of diseases, namely X-ray, computed tomography (CT), magnetic resonance imaging (MRI), positron emission tomography (PET), single photon emission computed tomography (SPECT), magnetic resonance imaging (MRI), functional magnetic resonance imaging (fMRI), magnetic resonance spectroscopy (MRS), mammography and diffusion tensor imaging (DTI). In early postmortem studies, brain volume is measured by the water displacement method (Witelson et al. 2006). However, nowadays, MRI is a precise noninvasive imaging technique which produces three-dimensional detailed normal and diseased anatomical

Communicated by Kannan.

✉ P. Kalavathi
pkalavathi.gri@gmail.com

T. Priya
suga.priya04@gmail.com

V. B. Surya Prasath
surya.iit@gmail.com; surya.prasath@cchmc.org;
prasatsa@uc.edu

R. Sivanesan
rsivanesan90@gmail.com

[1] Department of Computer Science and Applications, The Gandhigram Rural Institute (Deemed to be University), Gandhigram, Dindigul 624302, India

[2] Division of Biomedical Informatics, Cincinnati Children's Hospital Medical Center, Cincinnati, OH 45229, USA

[3] Department of Biomedical Informatics, College of Medicine, University of Cincinnati, Cincinnati, OH 45267, USA

[4] Department of Pediatrics, College of Medicine, University of Cincinnati, Cincinnati, OH 45267, USA

[5] Department of Electrical Engineering and Computer Science, University of Cincinnati, Cincinnati, OH 45221, USA

Published online: 11 February 2021

brain images, it clearly visualizes internal structures of brain tissue (WM, GM and CSF). Furthermore, it is used to estimate the volume of brain tissue in both qualitative and quantitative leads to identify different types of neurodegenerative disorders like Alzheimer's disease (AD), multiple sclerosis (MS), Parkinson's disease (PD), Huntington disease (HD) and Schizophrenia (SC).

AD (Alzheimer's Disease 2018; Brain Atrophy 2018) is the most common and fastest growing irreversible and progressive form of dementia deposits beta-amyloid plaques and neurofibrillary tangles. According to Clemenson et al., (Clemenson et al. 2017), AD has four progressive stages, preclinical, mild, moderate and severe stage (Alzheimer's disease 2019). It begins to spread throughout the brain and it slowly destroys healthy neuron, the hippocampus in the early stages and continuously affects the other cortical areas of the brain in the latter stages. Also, it shrinks the brain and loses the ability to communicate with one another and eventually affect memory, thinking skills and daily living activities. It causes severe health problem for the older population (Lella and Estrada 2020; Impedovo et al. 2019). Sample MR brain coronal slices before and after the occurrence of AD is shown in Fig. 1.

Detection of AD in MRI brain image is important in brain imaging applications for diagnosis and accurate in treatment planning. One approach for AD detection is to measure the reduction of brain tissue in WM, GM and CSF after segmenting it from the MR brain images and comparing with its respective brain tissue of normal images. The accurate AD classification can be done by measuring the volume difference of these segmented brain tissues with the standard volumes measures of cognitive normal (CN)/normal (N) patients. The reduction in the brain tissue (WM, GM and CSF) volume helps to identify different types of diseases including AD, MS, PD, HD and SC. Volume estimation of brain tissue is essential for a detailed quantitative brain analysis in order to diagnose, detect and classify abnormalities and for further treatment planning. The past studies/available literature on brain volume estimation related to detection of AD reveals the fact that there are only few numbers of brain volume measurements methods available and are not robust on brain volume estimation to accurately detect AD. Hence, an obvious need for the development of effective computational techniques for quantification of brain tissue to detect AD is realized.

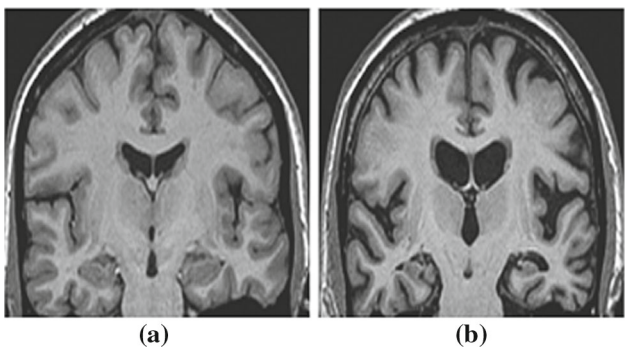

Fig. 1 MR brain coronal slices of a **a** Healthy, and **b** AD affected

A volume estimation of brain tissue based on the pixel counting-based method (PCBM) is presented in this paper. Since, by comparing the volumes of the segmented WM, GM and CSF of normal and AD images, the brain shrinkage can be quantified which help to detect and classify AD in MR brain images.

The remaining part of the paper is organized as follows: a study of different volume estimation methods from the literature is analyzed in Sect. 2, and brief description of methodology and existing automatic estimation method is described in Sect. 3 and Sect. 4, respectively. Section 5 describes results and discussion of different datasets, and finally conclusions are given in Sect. 6.

2 Review of literature

A study on the literature of AD detection techniques reveals the fact that only a limited number of researches have been carried out in the past. Ramaiah and Mohan (Ramaiah and Mohan 2011) proposed a pipelining process which contains different stages like normalization, ROI masks generation, segmentation and volume estimation using voxel-based morphometry (VBM5) and Snake Automatic Partition (itk-SnAP) tools for diagnosing different diseases related to changes in the brain tissue. Itk-SnAP works more robust in segmenting even small portions in a brain tissue. Suprijadi et al. (Pratama and Haryanto 2014) employed two methods of thresholding to segment the abnormality occurrence and estimated the tumor and stroke-attacked area in MRI images.

Smitha (Smitha et al. 2006) used weighted K-means clustering algorithm to segment various brain tissues. The volumes of the segmented tissues were then calculated and compared using the trapezoidal estimation method and Cavalieri's method. Klauschen et al. (Klauschen et al. 2009) compared the performances of SPM version 5, FSL and FreeSurfer (FS) in calculating GM volume (GMV), WM volume (WMV) and total brain volume (TBV) by using thin-section images. In order to detect, subtle changes in brain volume for clinical applications, Bresser et al. (Bresser et al. 2011) established methods such as Structural Image Evaluation using Normalization of Atrophy (SIENA), Unified Segmentation (US) and k-Nearest Neighbor (kNN)-based probabilistic segmentation and assessed its potential differences in precision and accuracy

and the results showed that US and kNN give good precision, accuracy and comparability for brain volume measurements. SIENA showed the best performance for measurements of volume change. A study of Heinen et al. (Heinen et al. 2016) deals with three methods of FS 5.3.0, SPM12 and FSL 5.0.7 for brain volume measurement of 1.5 and 3 T of T1-weighted images to determine robustness across different field strength. The results of these method show that FSL and FS are robust in calculating total brain volume (TBV), GM and WM than SPM, however, for intracranial volume (ICV), SPM is robust than FSL and FS. Accuracy for FS, SPM and FSL varies over different tissue compartments.

Kumazawa et al. (Kumazawa et al. 2010) introduced a method to measure the volumes of WM, GM and CSF based on the estimates of partial volume fractions for diffusion tensor magnetic resonance imaging (DTMRI) real data. Instead of assigning each voxel to a unique tissue type, each tissue type assigned within a voxel using a Maximum a Possibility (MAP) principle based on eigen values, apparent diffusion coefficient (ADC) and fractional anisotropy (FA). The results were then compared with the conventional hard segmentation methods. Modified MFCM by Anami and Unki (Anami and Unki 2014) segmented 100 different brain MRI images of both male and female into three tissue types, namely WM, GM and CSF, to estimate the percentage of CSF, WM and GM in the given brain image. Katuwal et al. (Katuwal et al. 2016) estimated brain volumes of GM, CSF and total intracranial volume (TIV) of T1-weighted MRIs of 417 autism spectrum disorder (ASD) subjects and 459 typically developing controls (TDC) from the ABIDE dataset using three popular preprocessing methods such as SPM, FMRIB Software Library (FSL) and FS, and the results emphasize the fact that ASD is higher than TDC with statistical significance but according to FSL and FS the differences were not significant. Further, regarding the validation, it indicates that SPM provides TIV estimates closest to manual segmentation followed by FS and then FSL.

Sargolzaei et al. (Sargolzaei et al. 2015) proposed a method includes two phases of analysis for estimation of ICV for two different groups of subjects with adult control (AC) and patients with Alzheimer's disease (AD). In the first phase, two types of operations are performed; the first operation is the measurements of ICV by FS, FSL and SPM are calculated and compared with the reference measurements by manually tracing ICV with the help of visual inspection. The second operation inter-operator variability analysis is performed with the same T1-weighted image volume of the subject and the intra-operator variability is analyzed by re-measuring the ICV which is done in the first operation. Intra-software reproducibility is also measured by repeatedly assigning automatic measurements of ICV using FS, FSL and SPM. The second phase of the study was implemented with similar processing power to keep the results unbiased from the potential unbalance processing units in software measurements and the results implied that FS showed promising estimates for both adult groups, whereas SPM showed more consistency in its ICV estimation over the different phases of the study.

According to the existing studies brain tissue volume can be estimated by two broad categories manual and automated techniques (Keller and Roberts 2009). In manual techniques, quantification of brain tissue volume is calculated by two methods, namely stereological with point counting and tracing methods. Stereological with the point counting method applied on randomly selected MR brain images with superimposing grid of points to estimate the area of interest and then counts all the points within the range. It leads to a complex problem for statisticians in predicting the precision regarding the observation of spatial dependence. Nevertheless one of the advantages of this method is that it is more efficient than tracing method in terms of time-consuming and labor intensive (Doherty et al. 2000) and it allows coefficient of error for identifying preliminary optimal parameters. In tracing method, to estimate the volume, the investigator is needed to trace the brain region of interest slice by slice and the points within the area are summed and multiplied the distance between successive traced regions. The main drawback of the method is that it takes a long time, while tracing and sometimes it can lead to identify non-brain tissues.

Automatic methods for estimating brain tissue volume are developed to reduce the human interference in estimation procedure. There are some widely estimated software packages available such as FS (Dale et al. 1999), FSL (Smith et al. 2004) and SPM (Ashburner and Friston 2005). These software packages do not require external intervention but sometimes default parameters were selected as required by the background algorithms. Further, these software packages have some drawbacks regarding precisely estimating brain volumes from MR imaging data. Often, before applying the automatic models that are available in these popular software packages, certain preprocessing steps have to be undertaken on the MR images, and it can lead to time-consuming fine-tuning of the associated parameters. However, previous studies on these packages imply that each tool performed well on each tissue types. In our proposed method, all the preprocessing processes are done normally and well executed on all the tissues types of MR brain images.

In this paper, the volume of the segmented brain tissue (WM, GM and CSF) is estimated using a pixel counting-based method (PCBM). The quantitative experiments were done using T1-weighted images from Minimum Interval Resonance Imaging in Alzheimer's Disease (MIRIAD), Alzheimer's Disease Neuroimaging Initiative (ADNI) and

two volumes of T1-weighted images, two volumes of T2-weighted real-time clinical images collected from a Scan center.

3 Methodology

Brain volume is also called as cranial capacity and it varies from person to person depending on several factors, such as age, environment and body size. It is also used as an adjustment factor on comparison of brain structures between cognitive normal (CN)/normal (N) patients. The volume is usually measured in centimeters (cm^3). Modern humans have cranial capacities from 950 to 1800 cm^3, but the average volume of a modern human brain is 1300 to 1500 cm^3volume (Brain Atrophy 2018). In order to measure the brain volume, we have used the pixel counting-based method (PCBM). It requires two major computations: (i) area calculation and (ii) Volume estimation for the segmented WM, GM and CSF in each brain slice of a volume. This is demonstrated as block diagram in Fig. 2.

In order to get accurate estimation of brain tissue, some preprocessing and proper segmentation of brain tissue is needed because these images are affected by noises during image acquisition and transmission process (Somasundaram and Kalavathi 2012a) and human head part such as skull, eye, marrow and skin part are also need to be removed. Many denoising and segmentation techniques are developed in recent studies (Kalavathi and Prasath 2015, 2016a, 2016b; Somasundaram and Kalavathi 2011, 2012b, 2012c; Kalavathi 2014; Kalavathi and Priya 2016) in the form of the edge-based method (Aslam et al. 2015), region growing-based method (Somasundaram and Kalavathi 2014; Kavitha and Chellamuthu 2013), cluster-based method (Chuwdhury et al. 2016; Kalavathi and Priya 2017a; Kalavathi et al. 2017b; Caponetti et al. 2017), entropy-based method (Kalavathi and Priya 2018a), threshold-based method (Kalavathi 2013; Somasundram and Kalavathi 2011; Kalavathi and Priya 2018b), classification-based method (Renjith et al. 2015) and color model-based method (Attique et al. 2012). Based on these techniques, we developed wavelet-based bivariate shrinkage method (WBBSM) (Kalavathi and Priya 2017) and used contour-based brain segmentation (Somasundaram and Kalavathi 2013) technique to remove noise and non-brain tissue from the images. The brain tissue in the input volume is segmented using Hue Saturation Value-Based Histogram Thresholding Technique (HSVBHTT) proposed in (Kalavathi and Priya (2019)). First of all, this method converts the preprocessed image into HSV color image. Then construct circular histogram of hue component and histogram of saturation and value. After that threshold values are calculated based on the circular histogram statistics ranging from 0° to 360°. The minimum and maximum value of each color channel is calculated. These values are considered as threshold value to obtain the color mask. The constructed color mask is overlaid on the preprocessed image to get the segmented result of brain tissue (CSF, GM and WM). Then, the tissue volumes are estimated using the proposed pixel counting-based method (PCBM) and it is compared with existing automatic estimation method namely the statistical parametric mapping (SPM).

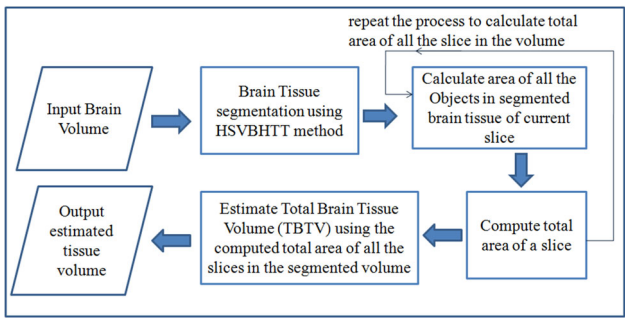

Fig. 2 Block diagram of the proposed pixel counting-based method (PCBM)

3.1 Calculation of brain tissue area

The segmented images of brain tissue WM, GM and CSF are taken separately as input and are then converted into a binary image. The area of each object in a slice is calculated by counting the number of white pixels. (A pixel with value 1 are considered as white and 0 are considered as black.) Then, we obtain the total area of a slice by Eq. (1).

$$\text{Area}_i = \sum_{O=1}^{O_i} \text{No. of White Pixel} * \text{Image Resolution}$$

where i is the ith slice and O_i is the number of objects in the ith slice, image resolution = Field of View (FOV)/matrix size, which will be specified in the selected datasets. Then, the total area of a slice is calculated by multiplying the slice thickness and slice gap. Slice gap (SG) is occurred during image acquisition process, and therefore, SG is considered for finding the area of a slice between the two adjacent slices using the following Eq. (2). This has been done separately for each brain tissue. The stack of slices denoting SG ad ST is illustrated in Fig. 3.

Fig. 3 Stacks of slices denoting slice thickness (ST) and slice gap (SG)

$$\text{Total Area of slice}_i = \text{Area}_i * (\text{ST} + \text{SG}) \quad (2)$$

where ST and SG are slice thickness and gap, respectively.

3.2 Computation of segmented brain tissue volume

To compute the segmented tissue volume of a brain image, we add the total area of all the slices in the segmented volume except the last slice, since the last slice does not include the slice gap. The total volume is computed as per following Eq. (3).

$$\text{TBTV} = \sum_{i=1}^{N-1} \text{Total Area of Slice}_i + (\text{Area}_N * \text{ST}) \quad (3)$$

where N is the total number of slices and area_N is the area of the Nth slice.

3.3 Algorithm for total brain tissue volume (TBTV) measurement

1: START
2: Set Slice Thickness (ST), Slice Gap (SG) as per the given input brain volume
3: Read the segmented brain tissue volume
4: Repeat the following steps for all the slices in the input segmented brain tissue volume.
5: Let i be the current slice
6: Assign $\text{Area}_i = 0$; Total White $\text{Pixel}_i = 0$
7: For K = 1 to O_i (Number of objects in the i^{th} slice)
8: begin
9: Total White Pixel_i= Total White Pixel_i+ Number of white pixels in the current object
10: End For
11: Area_i = Total White Pixel_i * Image Resolution
12: Compute the Total Area of a slice_i using the Equation (2).
13: After computing the Total area for all the slices in the segmented brain tissue, estimate the Total Brain Tissue Volume (TBTV) as per the equation given in Equation (3).
14: STOP

4 Materials used

4.1 Dataset-1

The images in the first dataset are retrieved from Minimum Interval Resonance Imaging in Alzheimer's Disease (MIRIADdataset 2016) database and it is given in Table 1. These entire scan images were conducted on the 1.5 T Sigma MRI scanners (GE Medical systems, Milwaukee, WI, USA). Three-dimensional T1-weighted images were acquired with an IR-FSPGR (Inversion Recovery prepared Fast Spoiled Gradient Recalled) sequence, field of view 24 cm, 256 × 256 matrix, slices of 124 with 1.5 mm coronal partitions, TR 15 ms, TE 5.4 ms, flip angle 15°, TI 650 ms.

4.2 Dataset-2

The second dataset was obtained from Alzheimer's Disease Neuroimaging Initiative (ADNI) (ADNIdataset 2016) which contains images of T1-weighted fast field echo MRI images of cognitive normal (CN) and Alzheimer's disease (AD) images. The slices are taken from standardization of annual 2 years 3 T Philips medical systems with TR = 2300 ms, TE = 4.6 ms, flip angle = 8–9°, thickness = 1.2 mm, 160–170 contiguous coronal slices, and in-plane resolution 0.94 × 0.94 mm2, FOV = 256–260 × 240 cm^2, matrix size = 256 × 256 cm^2 of Dataset-2 is given in Table 1.

4.3 Dataset-3

The images in the third datasets are real-time images collected from privately owned medical diagnostic clinical imaging center M/S SBC Scan Center located in Dindigul, Tamilnadu, India (Scans 2020), which contains four volumes of T2-weighted coronal slices with both normal and Alzheimer's disease image. The slices are taken from 1.5 T Siemens machines with a dimension of 305 × 448 pixels, slice thickness = 4.5 mm with 1.4 mm inter-slice gap. The

Table 1 Details of brain datasets used in our work

S.No	Dataset name	No. of volume	Slice range in each volume	Gender	Age	Total slices
1	MIRIAD	69 (N–23, AD–46)	1–124	31 Male, 38 Female	55–87 years	8556
2	ADNI	14 (CN–7, AD–7)	1–160, 170	8 Male, 6 Female	71–87 years	2380, 2240
3	Real-time images	4 (N–2, AD–2)	1–46	4 Female	34–55 years	184

N Normal, *AD* Alzheimer's Disease, *CN* Cognitive Normal

field of view read = 230 m, the field of view phase = 90.6%, the field of view fixed = 230 × 208, 4 mm, and dataset size is nearly 190 slices per volume for all the sequences. No expert segmented images are provided for this dataset. The descriptions of above three datasets are given in Table 1.

5 Results and discussion

The proposed brain tissue volume estimation method is applied on the segmented brain tissue of the selected datasets (Dataset-1 to Dataset-3). The brain tissue volume measurement for Dataset-1 to Dataset-3 is done by taking the specified ST and SG in the respective datasets. We applied the proposed method and existing automatic estimation method to find TBTV on Dataset-1 to Dataset-3 of CN / N and AD affected images to detect AD. The estimated volumes for the randomly selected brain volume of Dataset-1, Dataset-2 and Dataset-3 are given in Tables 2, 3. The corresponding 3D views of these selected volumes of CN / N and clinical are shown in Figs. 4 and 5, respectively,

In order to detect occurrence of AD in MR brain image, we have calculated the volume separately for these segmented tissues (WM, GM and CSF) and also estimated the total brain tissue volume for both CN / N and AD brain image from Dataset-1 to Dataset-3. In the datasets (Dataset-1 to Dataset-3), CN / N images are provided for the corresponding AD volumes to detect AD and for comparative analysis of these two volumes (CN/N and AD) to classify Alzheimer's disease. CN is not a part of AD and does not denote loss of neurons in the brain cells. It is a gradual variable change depicted in the brain MR image when a person enters into old age.

To test the efficiency of our proposed method, the existing state-of-the-art method statistical parameter mapping (SPM) proposed by Friston et al. (Friston et al. 2008) used for the analysis and estimation of brain imaging data sequences with general linear model and random field theory. This tool runs with default settings (Guo et al. 2019). In order to calculate brain tissue volume of WM, GM and CSF, Spm_get_volume script ((Ashburner and Friston 2000; SPM 2019)) was implemented with corresponding native space tissue maps because to minimize any volume changes due to spatial transformation. Finally, TBV was estimated as the sum of the GM, WM and CSF volumes with the native space of structural MRI. The estimated brain tissue volume by SPM for CN / N and AD brain image of Dataset-1 to Dataset-3 for the selected sample volumes is illustrated in Figs. 4, 5 as given in Table 2. The computed brain tissue volume by the proposed method for both selected sample CN / N and AD brain image from Dataset-1 to Dataset-3 (Figs. 4, 5) is given in Table 3.

From Tables 2 , 3 and Figs. 4, 5, it is observed that the computed brain tissue volumes of the segmented brain tissue of WM and GM of the CN/N brain are higher than the AD affected respective brain volume. In brain volume 3, and volume 4, the computed volume of CSF tissue of AD brain is higher than the CN/N. This is since, when a brain is affected with AD, shrinking occurs in the tissues, and when the shrinking happens on the inside of the brain volume; it is pronounced into black pixels in the resultant

Table 2 Estimation of brain tissue (WM, GM and CSF) volumes for the sample volumes of the selected dataset using existing technique statistical parametric method (SPM)

Volume label	Volume in cm^3 for CN/N brain				Volume in cm^3 for AD brain			
	WM	GM	CSF	TBV	WM	GM	CSF	TBV
Volume 1	313.528	814.378	180.977	1308.884	445.635	612.194	153.067	1210.898
Volume 2	454.205	563.036	359.493	1376.735	650.396	529.673	123.108	1279.351
Volume 3	592.595	752.273	102.988	1447.860	478.080	557.016	333.675	1368.771
Volume 4	514.792	795.989	105.740	1416.522	477.359	515.837	303.207	1326.393
Volume 5	455.404	578.184	364.585	1398.174	491.813	534.661	177.672	1204.147

CN Cognitive Normal, *N* Normal, *AD* Alzheimer's Disease

Table 3 Estimation of brain tissue (WM, GM and CSF) volumes for the sample volumes of the selected dataset using proposed pixel counting-based method (PCBM)

Volume label	Volume in cm^3 for CN/N brain				Volume in cm^3 for AD brain			
	WM	GM	CSF	TBV	WM	GM	CSF	TBV
Volume 1	534.576	660.572	301.785	1496.933	430.751	597.509	379.590	1387.850
Volume 2	398.780	926.309	172.656	1497.744	371.33.3	858.600	258.965	1488.897
Volume 3	436.438	689.106	365.824	1491.368	471.850	577.649	342.419	1391.918
Volume 4	495.206	613.326	370.691	1479.223	583.323	585.702	169.605	1338.630
Volume 5	681.507	626.027	119.871	1427.405	439.835	601.196	238.550	1279.580

CN Cognitive Normal, *N* Normal, *AD* Alzheimer's Disease

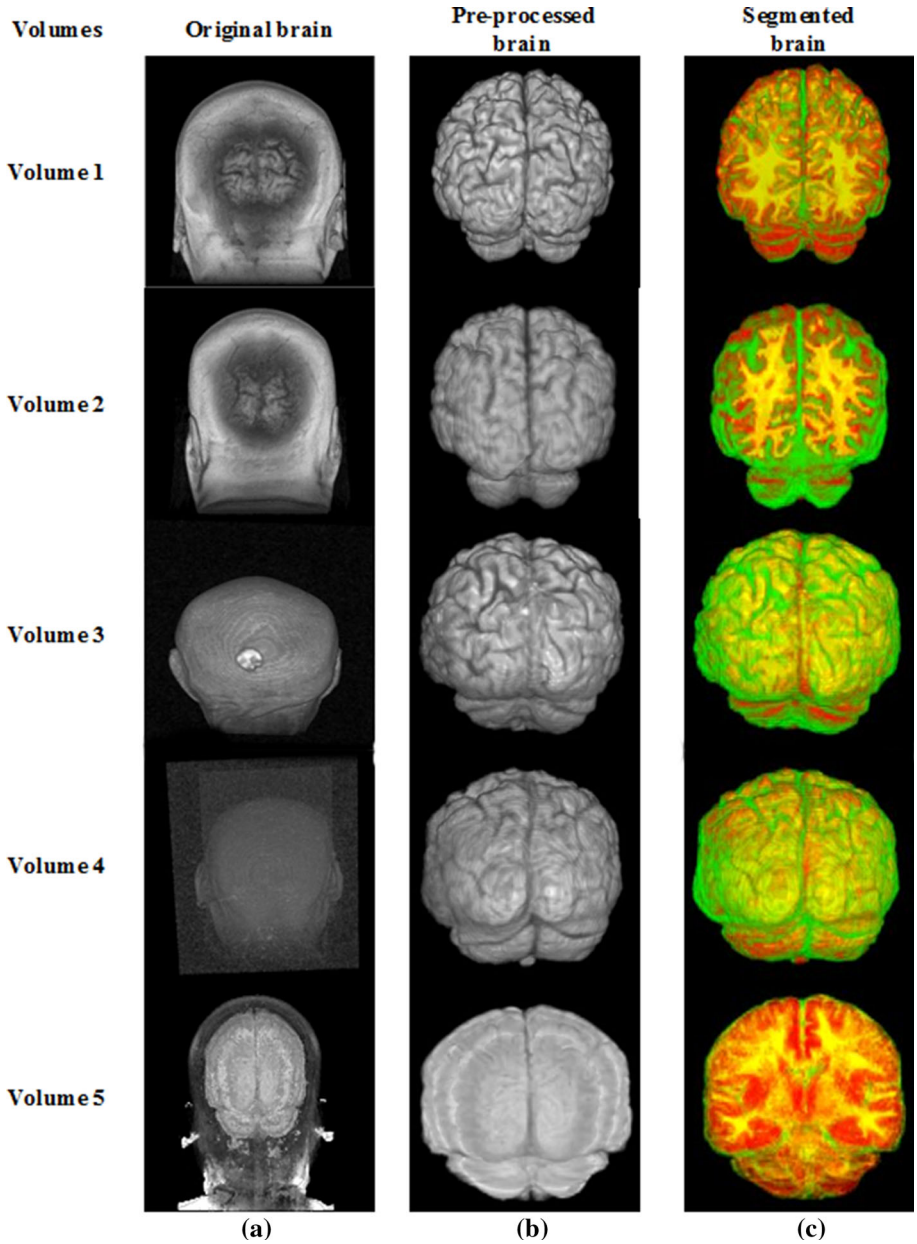

Fig. 4 3D view of cognitive normal/normal brain volume. **a** Original brain **b** Preprocessed brain **c** Segmented brain volume. Yellow denotes WM, red denotes GM, green denotes CSF

MR Image. During the segmentation of CSF tissue, this black area inside the brain is also considered as CSF tissue. For the volume 1, volume 2 and volume 5 in Table 2, the computed CSF volume in AD affected brain is lesser than the CN/N due to more shrinkage in the outer area of the brain. Thus, from this reduction (or) difference in the brain

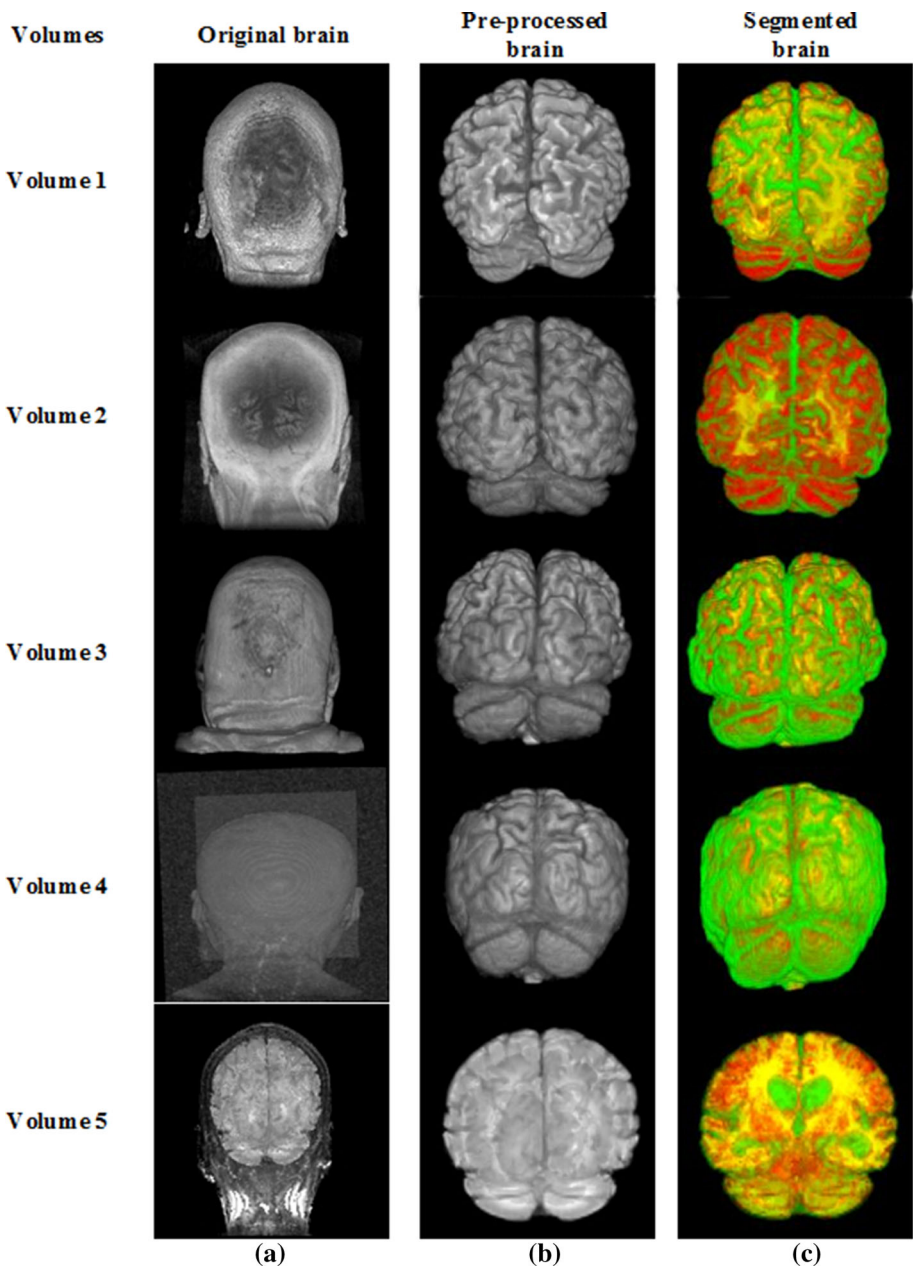

Fig. 5 3D view of AD affected brain volume. **a** Original brain **b** Preprocessed brain **c** Segmented brain volume. Yellow denotes WM, red denotes GM, green denotes CSF

tissue volumes of CN/N and AD affected brain, we can confirm that the brain is affected by AD. The severity/stage of AD can be classified according to the percentage of volume reduction in this tissue especially in WM and GM when compared to the CN/N volume. Similarly, it is observed from Table 3 that the computed tissue volumes of the segmented brain tissue of WM and GM of the CN/N brain are higher than the AD affected respective brain volume. Compared to SPM, the proposed PCBM gives better estimated values of brain tissue volume to classify the stages of AD.

From Tables 2 , 3 we notice that estimated brain tissue volumes of CN/N and AD affected brain of proposed PCBM method are higher than the existing automatic method SPM. The comparison of the estimated total brain tissues volume measures for the segmented WM, GM and CSF cognitive normal / normal and AD affected brain images using the proposed PCBM and the existing automatic estimation method SPM are shown in Figs. 6, 7 for the brain volume of Dataset—1 to Dataset—3, respectively.

From Figs. 6, 7, it is clearly evident that the performance of the proposed method PCBM on Dataset—1 to Dataset—3 of T1-weighted and T2-weighted cognitive normal / normal and AD affected brain images are more accurate when compared with SPM method. This can be witnessed

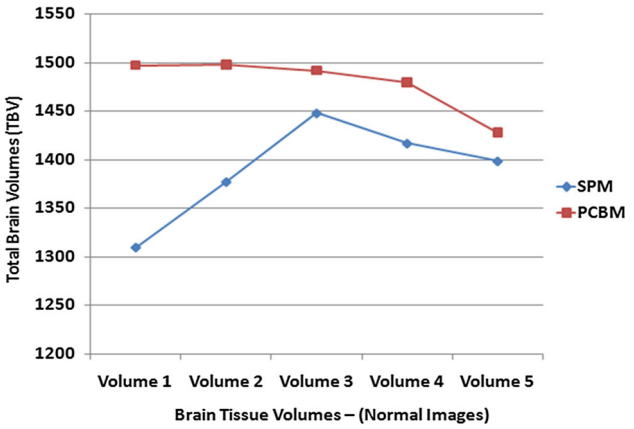

Fig. 6 Comparative analysis of computed TBV using statistical parameter mapping (SPM) with the proposed pixel counting-based method (PCBM) for Dataset—1–Dataset—3 of T1 and T2-weighted normal images

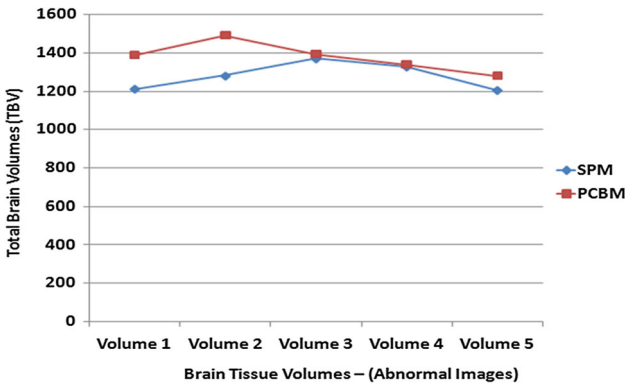

Fig. 7 Comparative analysis of computed TBV using statistical parameter mapping (SPM) with the proposed method PCBM for Dataset—1–Dataset—3 of T1 and T2-weighted abnormal images

by analyzing the computed TBV for the CN/N brain volumes by both the methods, the existing SPM and the proposed PCBM.

6 Conclusions

In this work, we presented an efficient method to estimate the volume of the segmented brain tissue in MR brain images based on pixel counting-based method (PCBM). The experimental results of our proposed approach on brain volume images are compared with existing automatic segmentation method such as the statistical parametric mapping (SPM) widely used in the literature. The shrinkage in the brain volumes is determined by considering the volume reduction in Alzheimer's disease (AD) brain compared to its CN/N volume. It is observed from the experimental results that our proposed method performs well compared to the existing method and it may thus can be used as an effective tool to detect AD in MR brain images.

Funding This study was funded by the Science and Engineering Research Board (SERB), Department of Science and Technology, Government of India. File NO. EEQ/2016/000375 (PK). VBSP is supported by NCATS/NIH grant U2CTR002818, NHLBI/NIH grant U24HL148865, NIAID/NIH grant U01AI150748, Cincinnati Children's Hospital Medical Center—Advanced Research Council (ARC) Grants 2018–2020, and the Cincinnati Children's Research Foundation—Center for Pediatric Genomics (CPG) grants 2019–2021.

Compliance with ethical standards

Conflict of interest The authors declare that they have no conflict of interest.

Ethical approval This article does not contain any studies with human participants performed by any of the authors.

References

ADNIdataset (2016) Available from: http://adni.loni.usc.edu/methods/mrianalysis/adni-standardized-data

Alzheimer's disease and related dementia's (2019): https://www.nia.nih.gov

Alzheimer's Disease (2018): http://www.snmmi.org/AboutSNMMI/Content.aspx?ItemNumber=9870

Anami BS, Unki PH (2014) A fuzzy C-means approach for tissue volume estimation in brain MRI images. Int J Computer Appl, Recent Adv Inf Technol 975:21–24

Ashburner J, Friston KJ (2000) Voxel based morphometry: the methods. NeuroImage 11(6):805–821

Ashburner J, Friston KJ (2005) Unified segmentation. Neuroimage 26:839–851. https://doi.org/10.1016/j.neuroimage.2005.02.018 (**PMID: 15955494**)

Aslam A, Khan E, and Beg MMS (2015) Improved edge detection algorithm for brain tumor segmentation. In: Second International Symposium on Computer Vision and the Internet (VisionNet), 58: 430–437. Elsevier

Attique M, Gilanie G, Ullah H, Mehmood MS, Naweed MS, Ikram M, Kamran JA, Vitkin A (2012) Colorization and automated segmentation of human T2 MR brain images for characterization of soft tissue. PLoS ONE 7(3):1–13

Brain Atrophy (2018): https://www.healthline.com/health/brain-atrophy#treatment

Bresser JD, Portegies MP, Leemans A, Biessels GJ, Kappelle LJ, Viergever MA (2011) A comparison of MR based segmentation methods for measuring brain atrophy progression. NeuroImage 54(2):760–768. https://doi.org/10.1016/j.neuroimage.2010.09.060

Caponetti L, Castellano G, Corsini V (2017) MR brain image segmentation: a framework to compare different clustering techniques. Information 8:138

Chuwdhury GS, Kkaliluzzaman Md, Mahfuz MdR, Al (2016) Analyzing wavelet and bidimensional empirical mode decomposition of MRI segmentation using fuzzy C-means clustering. Rajshahi Univ J Sci Eng 44:101–112

Clemenson D, Cung S, Kerns M, Quist R, and Rathi H, (2017) What is Alzheimer's disease: https://alzheimersdiseasebiol2095.wordpress.com

Dale AM, Fischl B, Sereno MI (1999) Cortical surface-based analysis: i Segmentation and surface reconstruction. Neuroimage 9(2):179–194

Doherty CP, Fitzsimons M, Holohan T, Mohamed HB, Farrell M, Meredith GE, Staunton H (2000) Accuracy and validity of stereology as a quantitative method for assessment of human temporal lobe volumes acquired my magnetic resonance imaging. Magn Reson Imag 18:1017–1025

Friston KJ, Holmes AP, Worsley KJ, Poline J-P, Frith CD, Frackowiak RSJ (2008) Statistical parametric maps in functional imaging: a general linear approach. Hum Brain Mapp 2(4):189–210. https://doi.org/10.1002/hbm.460020402

Guo C, Ferreira D, Fink K, Westman E, Granberg T (2019) Repeatability and reproducibility of FreeSurfer, FSL-SIENAX and SPM brain volumetric measurements and the effect of lesion filling in multiple sclerosis. Eur Radiol 29:1355–1364. https://doi.org/10.1007/s00330-018-5710-x

Heinen R, Bouvy WH, Mendrik AM, Viergever MA, Biessels GJ, de Bresser J (2016) Robustness of automated methods for brain volume measurements across different MRI field strengths. PLoS One 10:1–16. https://doi.org/10.1371/journal.pone.0165719

Impedovo D, Pirlo G, Vessio G, Angelillo MT (2019) A handwriting-based protocol for assessing neurodegenerative dementia. Cognitive Comput 11(4):576–586

Kalavathi P (2013) Brain tissue segmentation in MR brain images using Otsu's multiple thresholding technique. Proceeding IEEE ICCSE Conference, 639–642.

Kalavathi P (2014) Computation of brain asymmetry in 2D brain images. Int J Sci Eng Res 5(7):1167–1171

Kalavathi P, and Prasath VBS (2015) Adaptive nonlocal filtering for brain MRI restoration. International Symposium on Signal Processing and Intelligent Recognition Systems (SIRS), Trivandrum, India. Proc. in Springer AISC 425 (eds.: Thampi SM, Bandyopadhyay S, Krishnan S, Li KC, Mosin S, Ma M), 571–580

Kalavathi P, Prasath VBS (2016a) Methods on skull stripping of MRI head scan images - a review. J Digit Imag 29(3):365–379. https://doi.org/10.1007/s10278-015-9847-8

Kalavathi P, Prasath VBS (2016b) Automatic segmentation of cerebral hemispheres in MR human head scans. Int J Imag Syst Technol—Neuroimag Brain Map 26(1):15–23

Kalavathi P, and Priya T (2016) Removal of impulse noise using histogram based localized Wiener filter for MR brain image restoration. IEEE International Conference on Advances in Computer Applications (ICACA), 4–8

Kalavathi P, Priya T (2017) Noise removal in MR brain images using 2D wavelet based bivariate shrinkage method. Global J Pure Appl Math 13(5):77–86

Kalavathi P, and Priya T, (2017a) Segmentation of brain tissue in MR brain image using wavelet based image fusion with clustering techniques, In: Proceedings of National Conference on Computational Methods, Communication Techniques and Informatics, Gandhigram, Dindigul, India. Madurai: Shanlax Publications, 28–33.

Kalavathi P, Priya T (2018) Histogram based multimodal minimum cross entropy thresholding method for magnetic resonance brain tissue segmentation. J Comput Theor Nanosci 15(6/7):2430–2436. https://doi.org/10.1166/jctn.2018.7484

Kalavathi P, Priya T (2018) Brain extraction from MRI human head scans using outlier detection based morphological operation. Int J Computer Sci Eng 6(4):266–273

Kalavathi P, Priya T (2019) HSV based histogram thresholding technique for MRI brain tissue segmentation. In: Marques O, Krishnan S, Li KC, Ciuonzo D, Kolekar M, Thampi S (eds) Advances in signal processing and intelligent recognition systems. Springer CCIS, NY, pp 1–12

Kalavathi P, Arul Annis Chirsty A, Priya T (2017) Detection of alzheimer disease in MR brain images using FFCM method, computational methods communication techniques and informatics. Shanlax Publications, Madurai, pp 140–144

Katuwal GJ, Baum SA, Cahill ND, Dougherty CC, Evans E, Evans DW, Moore GJ, Michael AM (2016) Inter-method discrepancies in brain volume estimation may drive inconsistent findings in autism. Front Neurosci 10:439. https://doi.org/10.3389/fnins.2016.00439

Kavitha AR, Chellamuthu C (2013) Detection of brain tumor from MRI image using modified region growing and neural network. Imag Sci J 61(7):556–567

Keller SS, Roberts N (2009) Measurement of brain volume using MRI: software, techniques, choices and prerequisites. J Anthropol Sci 87:127–151

Klauschen F, Goldman A, Barra V, Meyer-Lindenberg A, Lundervold A (2009) Evaluation of automated brain MR image segmentation and volumetry methods. Hum Brain Mapp 30(4):1310–1327

Kumazawa S, Yoshiura T, Honda H, Toyofuku F, Higashida Y (2010) Partial volume estimation and segmentation of brain tissue based on diffusion tensor MRI. Med Phys 37(4):1482–1490

Lella E, Estrada E (2020) Communicability distance reveals hidden patterns of Alzheimer's disease. MIT Press J 4:4

MIRIADdataset (2016) Available from: http://miriad.drc.ion.ucl.ac.uk/atrophychallenge

Pratama SHS, Haryanto F (2014) Volume estimation of brain abnormalities in MRI data. AIP Conf Proc 1587:101. https://doi.org/10.1063/1.4866543

Ramaiah NP, and Mohan CK (2011) ROI-based tissue type extraction and volume estimation in 3D brain anatomy. International Conference on Image Information Processing, Shimla, India. IEEE, 1–5. doi:https://doi.org/10.1109/iciip.2011.6108941.

Renjith A, Manjula P, Kumar PM (2015) Brain tumor classification and abnormality detection using neuro-fuzzy technique and Otsu thresholding. J Med Eng Technol 23:1–10

Sargolzaei S, Sargolzaei A, Cabrerizo M, Chen G, Goryawala M, Noei S, Zhou Q, Duara R, Barker W, Adjouadi M (2015) A practical guideline for intracranial volume estimation in patients with alzheimer's disease. BMC Bioinform 16(Suppl 7):S8. https://doi.org/10.1186/1471-2105-16-s7-s8

SBC Scans (2020) Dindigul, State of Tamilnadu, India

Smith SM, Jenkinson M, Woolrich MW, Beckmann CF, Behrens TE, Johansen-Berg H (2004) Advances in functional and structural MR image analysis and implementation as FSL. NeuroImage 23:S208–S219. https://doi.org/10.1016/j.neuroimage.2004.07.051 (**PubMed PMID: 15501092**)

Smitha SS, Revathy K, and Chandrasekharan K (2006) Segmentation and volume estimation of brain tissues from MR images. In: Ao SI, Lee JA, Chaudhuri P, Feng DD (eds) Proceedings of the International Multi Conference of Engineers and Computer Scientists, Lecture Notes in Engineering and Computer Science, Hong Kong, China, Newswood Limited. 543–47.

Somasundaram K, Kalavathi P (2011) Skull stripping of MRI head scans based on Chan-Vese active contour model. Int J Know Manage E-learn 3(1):7–14

Somasundram K, Kalavathi P (2011) Medical image binarization using square wave representation. CCIS Springer, Berlin, pp 151–58

Somasundaram K, Kalavathi P (2012a) Analysis of imaging artifacts in MR brain images. Oriental J Comput Sci Technol 5:135–141

Somasundaram K, and Kalavathi P (2012b) Medical image denoising using Non-linear spatial mean filters for edge detection. Proceeding Signal and Image Processing, New Delhi, India, 149-154

Somasundaram K, and Kalavathi P (2012c) A novel skull stripping technique for T1-weighted MRI human head scans. Proceeding ICVGIP Conf, ACM Digital Library 1–8

Somasundaram K, Kalavathi P (2013) Contour-based brain segmentation method for magnetic resonance imaging human head scans. J Comput Assist Tomogr 37(3):353–368. https://doi.org/10.1097/RCT.0b013e3182888256

Somasundaram K, Kalavathi P (2014) Brain segmentation in magnetic resonance human head scans using multi-seeded region growing. Imag Sci J 62:273–284

SPM (2019): https://en.wikibooks.org/wiki/SPM/VBM

Volume of a human brain (2018): https://hypertextbook.com/facts/2001/ViktoriyaShchupak.shtml

Witelson SF, Beresh H, Kigar DL (2006) Intelligence and brain size in 100 postmortem brains: sex, lateralization and age factors. Brain 129(2):386–398